

The hydrophobic modification of kappa carrageenan microgel particles for the stabilisation of foams

Ellis, A.I.; Mills, T.b.; Norton, I.t; Norton-welch, A.b

DOI:

[10.1016/j.jcis.2018.11.091](https://doi.org/10.1016/j.jcis.2018.11.091)

License:

Creative Commons: Attribution-NonCommercial-NoDerivs (CC BY-NC-ND)

Document Version

Peer reviewed version

Citation for published version (Harvard):

Ellis, AL, Mills, TB, Norton, IT & Norton-welch, AB 2019, 'The hydrophobic modification of kappa carrageenan microgel particles for the stabilisation of foams', *Journal of Colloid and Interface Science*, vol. 538, pp. 165-173. <https://doi.org/10.1016/j.jcis.2018.11.091>

[Link to publication on Research at Birmingham portal](#)

Publisher Rights Statement:

Checked for eligibility 04/01/2019

Published in Colloid and Interface Science
<https://doi.org/10.1016/j.jcis.2018.11.091>

General rights

Unless a licence is specified above, all rights (including copyright and moral rights) in this document are retained by the authors and/or the copyright holders. The express permission of the copyright holder must be obtained for any use of this material other than for purposes permitted by law.

- Users may freely distribute the URL that is used to identify this publication.
- Users may download and/or print one copy of the publication from the University of Birmingham research portal for the purpose of private study or non-commercial research.
- User may use extracts from the document in line with the concept of 'fair dealing' under the Copyright, Designs and Patents Act 1988 (?)
- Users may not further distribute the material nor use it for the purposes of commercial gain.

Where a licence is displayed above, please note the terms and conditions of the licence govern your use of this document.

When citing, please reference the published version.

Take down policy

While the University of Birmingham exercises care and attention in making items available there are rare occasions when an item has been uploaded in error or has been deemed to be commercially or otherwise sensitive.

If you believe that this is the case for this document, please contact UBIRA@lists.bham.ac.uk providing details and we will remove access to the work immediately and investigate.

The hydrophobic modification of kappa carrageenan microgel particles for the stabilisation of foams

A. L. Ellis*, T. Mills, I. T. Norton, A. B. Norton-Welch

School of Chemical Engineering, University of Birmingham, Edgbaston, B15 2TT, UK

*Corresponding author. E-mail address: axe520@bham.ac.uk

Abstract

Hypothesis

Polysaccharides such as kappa carrageenan are often utilised in fat replacement techniques in the food industry. However, the structural role they can provide within a product is limited by their hydrophilic nature. Hydrophilic particles can be surface-activated by hydrophobic modification e.g. *in-situ* interaction with a surfactant. This can drastically improve foam stability by providing a structural barrier around bubble interfaces offering protection against disproportionation and coalescence. Hence, it should be possible to bind negatively charged kappa carrageenan particles with a cationic surfactant through electrostatic interaction, in order to alter their surface properties.

Experiments

Lauric arginate was mixed with kappa carrageenan microgel particles at various concentrations and the potential electrostatic interaction was studied using zeta potential, turbidity and rheological measurements. Mixtures were then aerated and foaming properties explored, in particular the location of the particles.

Findings

25 Lauric arginate was successfully bound to kappa carrageenan microgel particles.
26 Consequently, particles were surface-activated and adsorbed at the air/water interface, as
27 shown by optical and confocal microscopy. Foam half-life peaked at an intermediate
28 surfactant concentration, where there was sufficient surfactant to coat particle surfaces but
29 the concentration was low enough to prevent the formation of large aggregates unable to
30 adsorb at the a/w interfaces.

31 [Keywords](#)

32 Microgel

33 Fluid gel

34 Particles

35 Biopolymer

36 Surface-activation

37 Foam

38 Pickering stabilization

39 1 Introduction

40 Aqueous foams are thermodynamically unstable systems, which collapse via liquid drainage,
41 disproportionation and coalescence. Surfactants provide limited stability against these
42 mechanisms by lowering the surface tension [1]. Foam stability can be dramatically
43 improved via the adsorption of particles to the air/water (a/w) interface, termed Pickering
44 stabilisation [2], which provides a structural barrier to coalescence and disproportionation
45 [3]. Particles need to have intermediate hydrophobicity and be partially wetted in order to
46 adsorb at an interface. Hydrophilic particles therefore need to be modified, typically either
47 by chemical modification or *in situ* modification with surfactants. There are many examples
48 of particle-surfactant combinations used to stabilise foams in the literature, a few of which
49 are: laponite clay particles with hexylamine [4], alkylammonium bromides [5] or CTAB [6],
50 alumina particles with short chain carboxylic acids [7] and calcium carbonate particles with
51 SDS [8]. However, none of these combinations are suitable for food-grade systems. There
52 are several reviews on food-grade particles for Pickering stabilisation but these mainly focus
53 on emulsion systems [9-11] and those that do investigate foams [12, 13] have generally not
54 studied particle-surfactant combinations. Recently however, Binks, Muijlwijk [14] have
55 studied the modification of calcium carbonate particles with various anionic surfactants for
56 potential use in food systems. The modification of hydrophilic particles using surfactants *in-*
57 *situ* is therefore an exciting emerging area of research for the food industry, which is only
58 just starting to be utilised.

59

60 One of the major challenges facing the food industry is the increasing Government and
61 consumer pressure to reduce the levels of fat in food products. Diets high in fat, especially
62 the saturated kind, can lead to high cholesterol and increase the risk of heart disease [15].

63 Polysaccharides are commonly used in fat replacement techniques. As well as their low cost
64 and high abundance, they have the ability to structure water [16-18] and mimic the
65 structural characteristics of oil droplets when in particulate form [19]. This has been enabled
66 by the development of fluid gels; suspensions of gelled particles dispersed in a non-gelled
67 continuous phase [20]. In addition, as many polysaccharides can be classified as vegan, their
68 use in reduced fat systems is of strong interest to the food industry as the demand for vegan
69 products escalates [21].

70

71 However, the hydrophilic nature of polysaccharides limits their use in food product
72 microstructure design. Hydrophobic modification and subsequent potential surface
73 activation of polysaccharide particles would therefore significantly increase their
74 functionality in such products, for example by enabling them to adopt a more important
75 structural role (similar to that of fat droplets in whipped cream [22]). The majority of
76 polysaccharides used in the food industry are anionic e.g. carrageenan, alginate, pectin and
77 xanthan. A cationic surfactant would therefore be required for potential electrostatic
78 interaction and subsequent surface-activation. Lauric arginate (LA) is one such surfactant,
79 which has been approved as generally regarded as safe (GRAS) within the United States for
80 certain food applications [23]. There are a small number of studies in the literature that
81 focus on the interaction between LA and anionic biopolymers; Bonnaud, Weiss [24] describe
82 a strong binding interaction between LA and anionic biopolymers pectin, alginate,
83 carrageenan and xanthan, indicated by isothermal titration calorimetry. Asker, Weiss [25]
84 suggest that the addition of pectin to mixed LA/Tween 20 micelles leads to the formation of
85 electrostatic complexes that have potential applications as functional ingredients. However,
86 to the best of the authors' knowledge, this is the first study that investigates the potential

87 surface-activation of polysaccharide particles through binding of LA for use in aqueous
88 foams.
89
90 Kappa carrageenan (κ C) was selected as the polysaccharide to study and was prepared in
91 fluid gel form in order to create microgel particles. It was chosen because firstly, it is
92 strongly negatively charged and so has a high potential for electrostatic interaction with LA
93 and secondly, microgels have shown interesting interfacial behaviour, primarily the ability to
94 deform upon adsorption to an interface. Microgels are an increasingly interesting area of
95 research due to their vast potential as colloidal building blocks and stabilising agents due to
96 their deformability, surface activity, reversible swelling behaviour and responsiveness to pH
97 and temperature [26]. A number of studies have demonstrated the ability of microgels to
98 adsorb to a fluid or a/w interface by diffusion-limited adsorption and subsequently deform
99 in order to maximise exposure [27-30]. Furthermore, Dickinson [26] recently highlighted the
100 significant, novel potential of biopolymer-based microgels to stabilise food emulsions and
101 foams.

102 2 Materials and methods

103 2.1 Materials

104 Kappa carrageenan (22048) and Tween 20 ($\leq 3.0\%$ impurities) were purchased from Sigma
105 Aldrich (UK). Lauric Arginate was obtained in the form of Cytoguard LA 2X (A&B Ingredients,
106 USA) in a liquid form with propylene glycol carrier and a 20% content of Lauric Arginate. All
107 were used without further purification and concentrations were calculated as weight
108 percentage.

109 2.2 Preparation of fluid gel

110 Kappa carrageenan (1 wt%) was dispersed in deionised water at room temperature, then
111 heated to 70 °C. The solution was transferred into a cooled jacketed pin stirrer through a
112 peristaltic pump at 70 °C. The outlet temperature was controlled to 5 °C to ensure gelation
113 occurred under shear (gelation temperature ≈ 25 °C). A retention time of 7.5 min was
114 achieved through using a pump speed of 20 mLmin⁻¹, resulting in a cooling rate of 8 °Cmin⁻¹.
115 The shaft rotation speed was set to 1500 rpm to give a narrow distribution of particle size
116 [31]. Fluid gels were stored at 5 °C.

117 2.3 Preparation of κ C fluid gel-LA complexes

118 1% κ C fluid gel was diluted 1:1 with deionised water. LA at various concentrations was then
119 added to the solution whilst stirring for 5 days at room temperature.

120 2.4 Zeta potential measurements

121 Zeta potential was determined using a Zetasizer (Malvern Instruments, UK) at 25 °C. κ C fluid
122 gel was diluted and its pH was altered from 1.5 to 10 using either NaOH or HCl of 1M
123 concentrations. Complexes were measured at their natural pH. All data points were carried
124 out in three replicates.

125 2.5 Turbidity measurements

126 The turbidity of κ C fluid gel-LA complexes was inferred from the absorbance at 600 nm
127 using a UV-Vis spectrophotometer (Orion AquaMate, Thermoscientific, UK) in 1 cm cuvettes
128 against deionised water. Measurements were carried out at 25 °C in three replicates.

155 2.6 Rheology

156 A Kinexus rheometer (Malvern Instruments, UK) was used to perform rheological
157 measurements at 25 °C. κ C fluid gel-LA complexes were tested after 24 h to ensure post-
158 production particle ordering completion [32, 33]. All measurements were conducted using a
159 serrated parallel plate of 60 mm diameter set to a 1 mm gap. Amplitude sweeps were
160 conducted at a frequency of 1 Hz as a function of applied oscillatory strain. All experiments
161 were carried out in three replicates.

162 2.7 Surface tension

163 Surface tension measurements of κ C fluid gel-LA complexes and LA solutions were
164 performed using a Kruss GmbH K100 tensiometer (Hamburg, Germany). The Wilhelmy plate
165 method was used to measure static surface tension at an immersion depth of 2mm at 25 °C.
166 Experiments were carried out in three replicates. The critical micelle concentration (CMC)
167 was calculated as the concentration at which surface tension stopped decreasing (Figure 6),
168 which was 0.15 wt% for LA solutions. This was similar to values reported in the literature:
169 0.18-0.21 wt% [24, 34]. The slight difference may have been a result of a difference in the
170 source of Lauric Arginate or in the method of obtaining CMC as isothermal titration
171 calorimetry was used in the referenced literature.

172 2.8 Aeration

173 κ C fluid gel-LA complexes of equal volumes were aerated using a Hobart mixing unit. The
174 highest speed setting was used for 7 min as this ensured air fraction was high for all systems

175 (between 0.65-0.95: the wet foam boundary). Air fraction was determined to assess foam
176 ability using Equation 1, by weighting equivalent volumes of fluid gel and foam, using three
177 replicates.

$$178 \text{ Air fraction} = 1 - \left(\frac{m_{\text{foam}}}{m_{\text{fluid gel}}} \right) \quad \text{Equation (1)}$$

179 Overall foam stability was measured using half-life measurements, that is the time taken to
180 reduce the height of the foam by half. The reduction of the foam height was recorded using
181 a CCD camera and the half-life was later calculated for three replicates (three separate
182 batches).

183 2.9 Liquid drainage and foam structure measurements

184 Liquid drainage and bubble size measurements were conducted using a Krüss DFA100LCM
185 foam analyser (Krüss, Germany). The κC fluid gel-LA mixture was poured into the foam cell
186 to cover the reference electrode followed by the externally produced foam. The decrease in
187 liquid fraction was then recorded using electrical conductivity measurements at 7 pairs of
188 electrodes along the cell height. Drainage profiles were recorded at sensor 3 (positioned at
189 half the foam height) for the first four hours from initial aeration. Bubble sizes were
190 recorded using a high resolution camera at a similar foam height. Experiments were carried
191 out in three replicates (three separate batches).

192 2.10 Optical microscopy

193 Aerated κC fluid gel-LA complexes were imaged using phase contrast microscopy (Leica
194 Microsystems, UK). The sample was placed onto a microscope slide with a coverslip and
195 observed using objective lenses up to 40x magnification.

196 2.11 Confocal microscopy

197 The microstructure of aerated κ C fluid gel-LA complexes as well as κ C fluid gel particles
198 before complexation (1 wt% κ C) were visualised using a confocal scanning laser microscope
199 (Leica TCS SPE, Heidelberg, Germany). The κ C fluid gel-LA complexes were aerated, placed
200 onto a microscope slide and stained with 0.01 wt% rhodamine B (Sigma Aldrich, Dorset UK).
201 A coverslip was then placed over the sample and a laser operating at a wavelength of 532
202 nm was used for imaging.

203 3 Results and Discussion

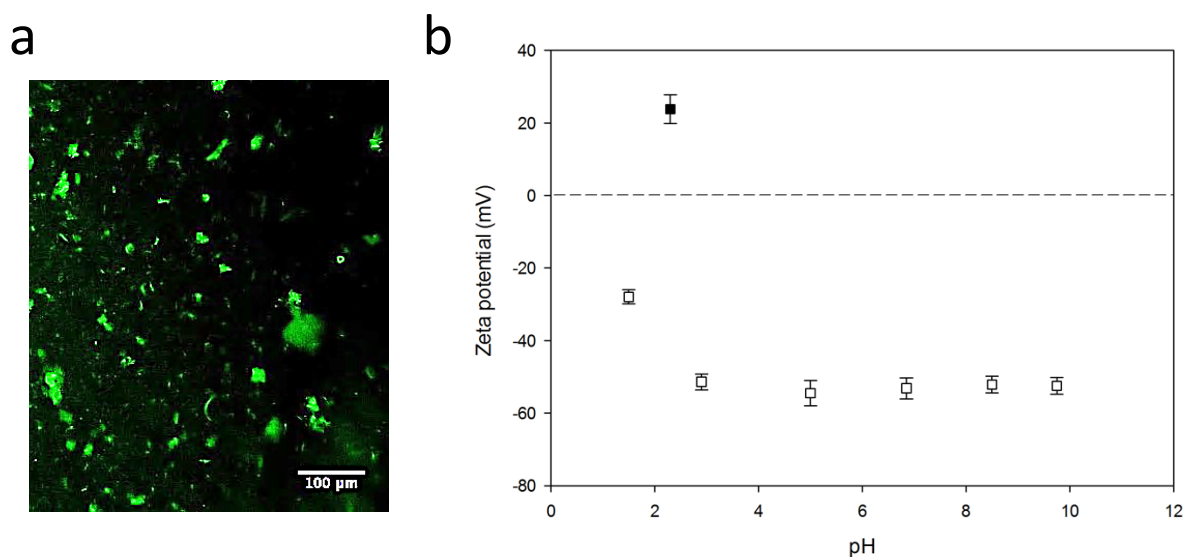
204 3.1 Production and characterisation of kappa carrageenan fluid gel

205 The gelling mechanism of kappa carrageenan (κ C) is widely accepted as a thermally-
206 reversible coil-to-helix transition followed by helix aggregation in the presence of K^+ ions
207 [35]. During fluid gel preparation, this process occurs under shear resulting in the
208 production of gel particles dispersed in a continuous phase, typically water [20]. The κ C
209 particles behave as soft microgel particles with penetrable “hairy” chains allowing for
210 particle overlap and interaction [36]. A fluid gel was produced at 1 wt% by shearing a hot
211 solution of κ C whilst it underwent gelation in a cooled jacketed pin stirrer at a shaft rotation
212 speed of 1500 rpm. Garrec, Guthrie [36] previously estimated the κ C fluid gel particle
213 volume fraction at 1 wt% as 0.65, here the fluid gel was diluted by half in order to study a
214 less concentrated suspension. Unfortunately, the particles cannot be visualised using optical
215 microscopy as the refractive index of κ C is too close to that of the water continuous phase
216 (1.334). However, particles could be imaged using confocal microscopy (Figure 1a), particle
217 diameter appeared to be in the 10-50 μ m range.

218

219 The zeta (ζ) potential of a diluted 1% kappa carrageenan (κ C) fluid gel was measured over a
220 pH range. At natural pH (6.8), ζ -potential was -53.1 ± 2.9 mV (Figure 1b), indicating κ C
221 particles were strongly negatively charged. This can be attributed to their ester sulphate
222 groups. ζ -potential remained constant over a wide pH range, only changing considerably at
223 pH 1.5 where particles became less negatively charged due to protonation of κ C under
224 strong acidic conditions (Figure 1b). The ζ -potential of Lauric arginate (LA) at natural pH
225 (2.3) was $+23.8 \pm 3.9$ mV, which confirmed its positive charge (Figure 1b). The potential

226 electrostatic interaction between κ C and LA was therefore investigated at their natural pH
227 and as a function of LA concentration.



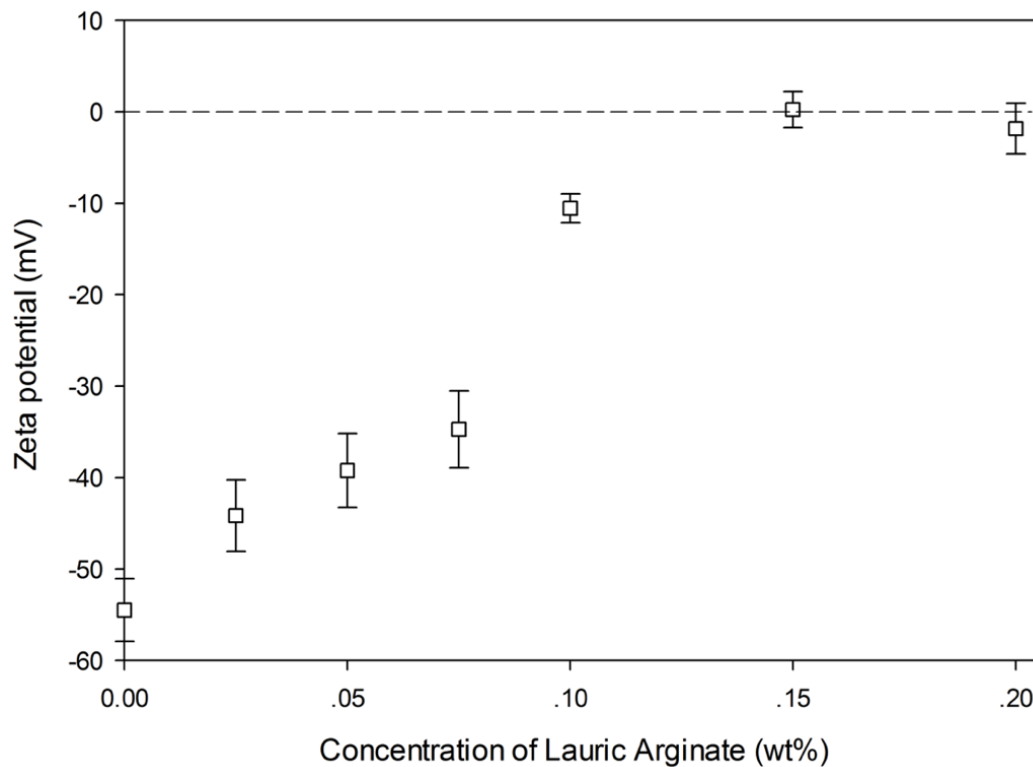
228
229 *Figure 1: (a) Confocal micrograph of diluted 1 wt% κ C fluid gel particles at natural pH (6.8) dyed with rhodamine B. (b) Zeta*
230 *potential measurements of diluted 1 wt% κ C fluid gel (\square) over a pH range and of LA at natural pH (\blacksquare).*

231

232 3.2 Complex formation through surfactant binding

233 LA was added at various concentrations to a diluted 1% κ C fluid gel solution. Zeta potential,
234 turbidity and rheological measurements were used to analyse the interaction. The ζ -
235 potential of κ C particles were measured 24 h after production. At 0% LA, ζ -potential was -
236 53.1 ± 2.9 mV, reflecting its negatively charged ester sulphate groups. Upon increasing LA
237 concentration, ζ -potential became increasing less negative until it reached zero at 0.15% LA
238 (Figure 2). This suggests that monomers of LA were binding to κ C particles reducing their
239 negative charge and at 0.15% LA, sufficient surfactant had been added to neutralise the
240 charge. The electrostatic interaction was facilitated by the cationic head group (L-arginine)
241 of LA and the negatively charged sulphate groups of κ C particles. It has often been reported
242 in the literature that the ζ -potential of negatively charged particles mixed with cationic
243 surfactants continued to increase with surfactant concentration after this charge
244 neutralisation had occurred [5, 8, 37]. This was a result of a second layer of surfactant

245 adsorbing onto the initial monolayer through hydrophobic interactions. However, increasing
246 the concentration of LA beyond 0.15% (to 0.2%) revealed a decrease in ζ -potential to $-3.8 \pm$
247 1.8 mV. A return to a negative ζ -potential suggests that a bilayer of surfactant cannot form
248 and instead added surfactant is most likely residing in the continuous phase.



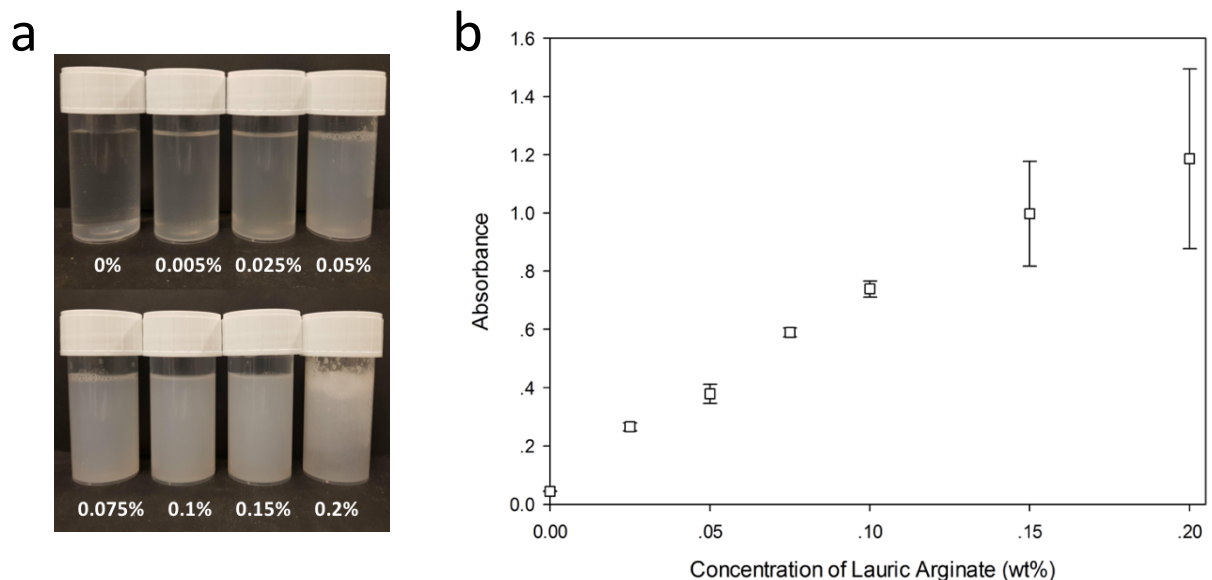
249

250 *Figure 2: Zeta potential measurements of κ C fluid gel particles as a function of increasing LA concentration. Concentration*
251 *is calculated as wt% of the total solution.*

252

253 Visible observations of κ C fluid gel + LA solutions confirmed a change in their structure with
254 increasing LA concentration (Figure 3a). Solutions increased in turbidity but remained
255 homogenous in appearance until 0.1% LA. From 0.1% LA increasingly large aggregates were
256 observed using optical microscopy, ranging from 100 μ m to 300 μ m in size. Turbidity was
257 measured using a UV-Vis spectrophotometer to quantify these observations. Absorbance
258 can be seen to increase linearly with LA concentration (Figure 3b). At 0.15% and 0.2% LA,
259 the error bars in absorbance data were considerably larger, due to substantial aggregates
260 observed in the solutions. This turbidity data provides further evidence of complex

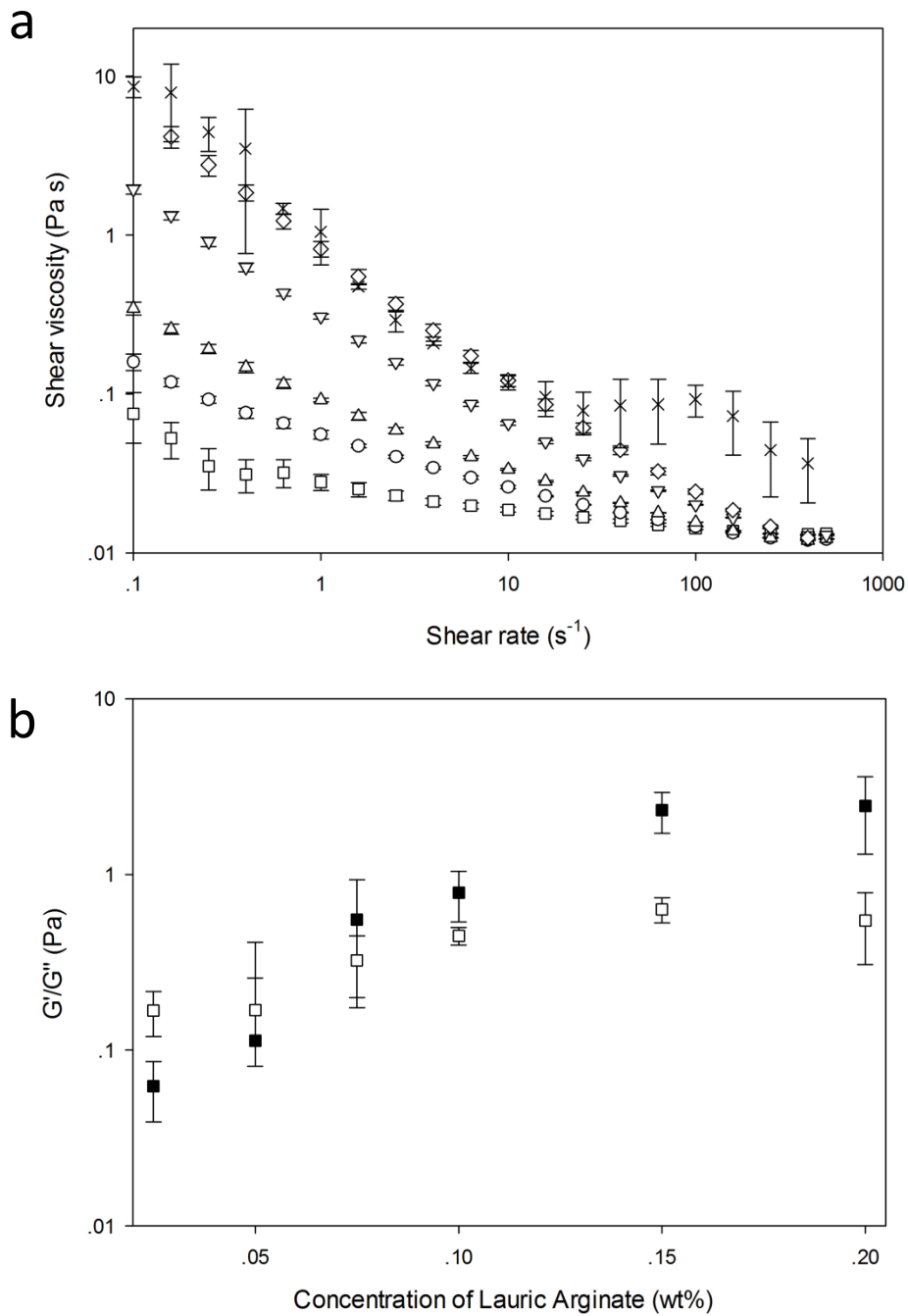
261 formation, where an increase in turbidity (scattering of light by particles) corresponds to an
262 increase in particle density, due to electrostatically bound surfactant. It is also clear that
263 aggregation of the complexes occurred, especially at higher LA concentrations. This was
264 caused by a reduction in particle charge, which led to less repulsion and therefore more
265 intermolecular interactions between particles. This effect was heightened at 0.15% LA and
266 0.2% LA as charge neutralisation of the complexes considerably limited their solubility. A
267 similar trend was first observed by Bonnaud, Weiss [24] where turbidity initially increased at
268 low concentrations of LA when mixed with iota-carrageenan, indicating the formation of
269 complexes. Larger aggregates were then observed at concentrations of 0.03-0.23 wt% LA.



270
271 *Figure 3: (a) Photographs of solutions of κ C fluid gel particles mixed with LA at various concentrations. (b) Absorbance of*
272 *the same solutions, measured using a UV-Vis spectrophotometer.*

273
274 The bulk viscosity of foams affect the mobility of the continuous phase and therefore
275 drainage velocity [38]. It is therefore essential to understand the rheological responses of
276 these fluid gels to understand how they behave when aerated. The viscosity profiles of κ C
277 fluid gel complexes at various LA concentrations were measured (Figure 4a). The flow curves
278 at all LA concentrations exhibited strongly shear thinning behaviour. This is typical of fluid

279 gels at low volume fractions, where they behave as highly aggregated suspensions
280 dominated mainly by colloidal forces [39]. At higher volume fractions, particles behave as
281 soft microgels where rheology is dependent on particle elastic modulus as well as particle-
282 particle interactions [32, 40]. From Figure 4a, at low shear rates a difference in fluid gel
283 viscosity can be observed, where it increased with LA concentration. However at high shear
284 rates, most fluid gels displayed a similar viscosity. This further confirms the difference in
285 particle aggregation. Initially, particles were aggregated together to various extents, but upon
286 shearing, the interactions between particles were broken and structures were similar. The
287 flow curve of 0.2% LA was different at higher shear rates, where it appears to shear thicken
288 at $\sim 50 \text{ s}^{-1}$, this was likely due to the larger aggregates jamming in the geometry. The
289 viscoelastic behaviour of the fluid gels was measured using oscillatory rheological data
290 (Figure 4b). At LA concentrations up to 0.1%, the loss modulus (G'') dominated over the
291 storage modulus (G') indicating a more viscous response from the system. However, at
292 0.15% and 0.2% LA, G' was dominant, which reflects a more elastic response. These
293 structures also exhibited a yield stress. Therefore, as aggregation of the particles increased
294 due to increased surfactant binding, a network with gel-like properties began to form,
295 leading to an eventual dominance in G' .



296

297

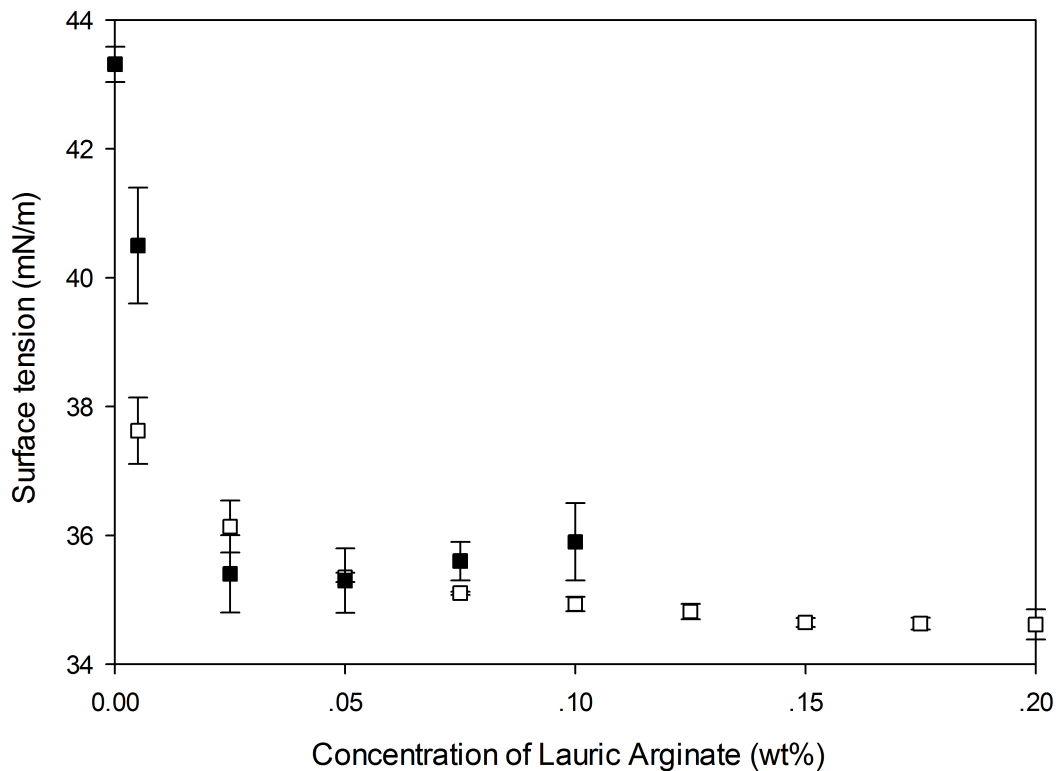
298

299

Figure 4: (a) shear viscosity of 1 wt% κ C fluid gel mixed with LA at 0.025% (\square), 0.05% (\circ), 0.075% (\triangle), 0.1% (∇), 0.15% (\diamond) and 0.2% (\times). (b) storage modulus (\square) and loss modulus (\blacksquare) of 1 wt% κ C fluid gel mixed with LA as a function of LA concentration.

300 3.3 Surface activity

301 The functionality of LA as a surfactant depends on its ability to adsorb at the a/w interface,
302 lowering the surface tension and stabilising the newly formed interface. In order to
303 investigate the surface-activity of κ C-LA complexes, equilibrium surface tension was
304 measured and compared to that of pure surfactant solutions (Figure 5). The surface tension
305 of pure LA solution decreased with concentration reaching a plateau at 0.15% LA with a
306 value of $34.6 \pm 0.07 \text{ mNm}^{-1}$. This is therefore its critical micelle concentration (CMC); above
307 this concentration, all additional surfactant monomers added to the system form micelles.
308 The surface tension of the complexes were then measured as a function of LA concentration
309 and compared to the pure surfactant solutions. The surface tension of pure kappa
310 carrageenan was $43.4 \pm 0.3 \text{ mNm}^{-1}$ (Figure 5). Upon addition of LA, the surface tension
311 quickly began to decrease until it plateaued at $35.0 \pm 0.6 \text{ mNm}^{-1}$ at 0.025% LA. It then
312 appeared to increase slightly at 0.1% LA. This is thought to be a result of the formation of
313 aggregates affecting the measurements. Above 0.1% LA, the aggregates increased in size
314 resulting in unreliable measurements. In surfactant-particle systems, the surface tension is
315 often lower than that of corresponding surfactant solutions [41]. It has been suggested that
316 particles act as surfactant carriers, thus increasing the concentration of surfactant at the
317 a/w interface [7] and that the size of the particles (dependent on individual systems)
318 determines the extent to which the surface tension is lowered [42]. Particle-surfactant
319 systems here exhibited similar surface tension values to the surfactant solutions (Figure 5).
320 The aqueous conditions, as well as size and shape of the particles may have therefore not
321 been optimal to cause a lowering of surface tension.



322

323 *Figure 5: Surface tension measurements as a function of LA for pure LA solutions (□) and κC-LA complexes (■).*

324 3.4 Aeration of surface-activated kappa carrageenan fluid gels

325 The ability of κC-LA complexes to incorporate air was determined using foam air fraction

326 measurements and compared to those of pure surfactant solutions. Systems were aerated

327 in a Hobart mixer for 7 minutes, which ensured that the air fraction was high. The air

328 fraction of pure surfactant solutions quickly reached a constant of around 0.97 upon

329 increasing LA concentration (Figure 6a). Foam capacity was high above and below the CMC

330 suggesting the method of foaming allowed equilibrium surface tension to be reached. The

331 air fraction of aerated κC-LA complexes followed a similar trend but values were slightly

332 lower than those of the pure surfactant solutions (~ 0.86). This was likely a result of

333 increased viscosity preventing the incorporation of as much air into the system. In addition,

334 Lesov, Tcholakova [43] have reported that foam air volume is also dependent on the

335 mechanism of stabilisation as well as solution viscosity, specifically the Pickering stabilised

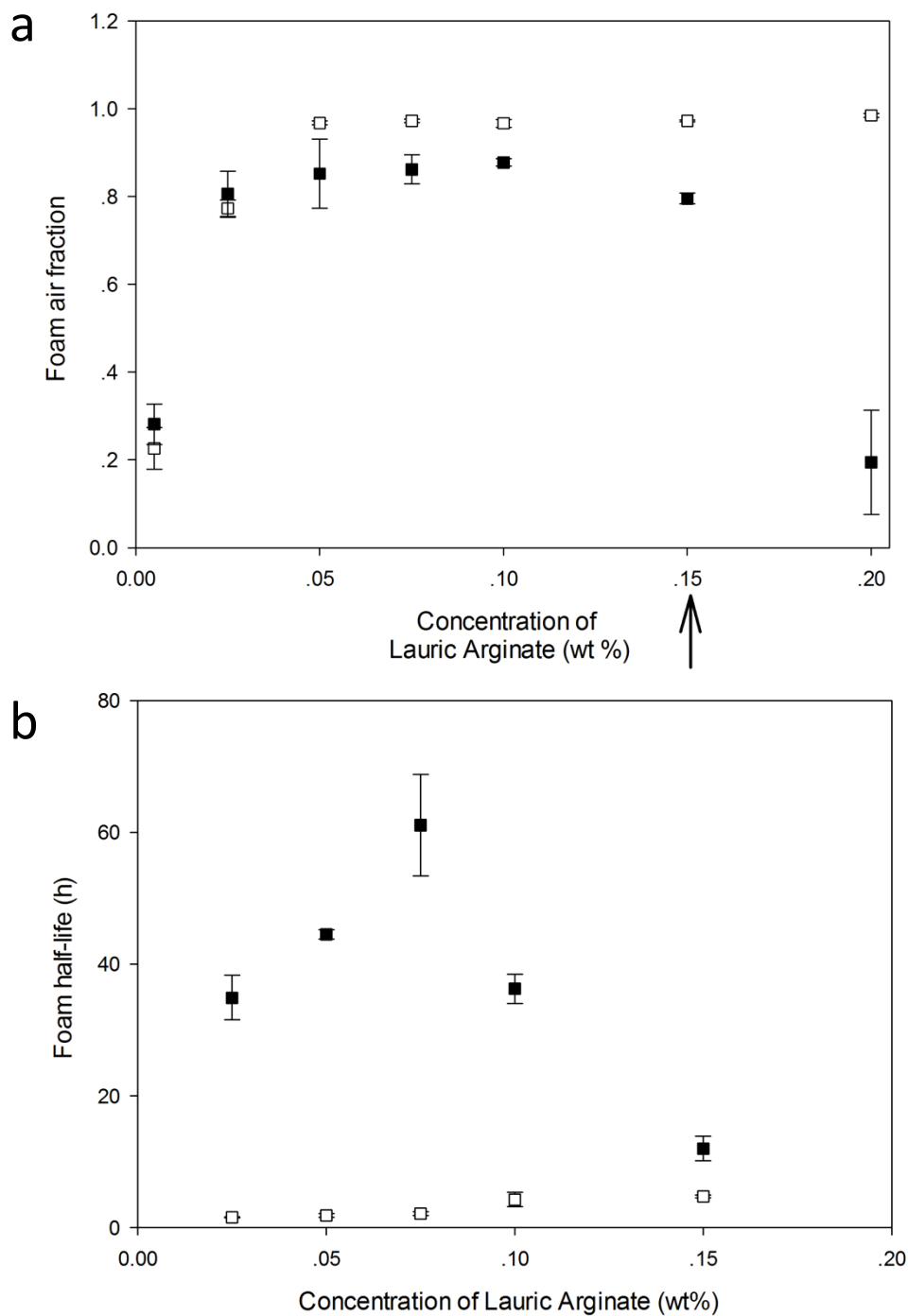
336 foams they studied had a lower air fraction when compared to surfactant-stabilised foams

337 of similar suspension viscosities. At 0.15% and more substantially, 0.2% LA, the air fraction
338 decreased. This was likely an effect of high particle aggregation and increased particle
339 density, as observed by turbidity and rheology measurements, which sterically hindered the
340 action of the surfactant. In addition, it was likely dense particles bridged and consequently
341 ruptured bubble interfaces as they were generated, preventing the growth of the foam
342 structure.

343

344 In order to investigate the potential Pickering stabilisation action of newly-formed κ C-LA
345 complexes, foam stability was explored. Firstly, foam half-life was measured and compared
346 to those of pure surfactant solutions (Figure 6b). Foams produced at 0.005% and 0.2% LA
347 were not measured as the air fraction was too low. Foam half-life initially increased from 35
348 ± 3 h at 0.025% LA up to 61 ± 8 h at 0.075% LA, where it peaked before decreasing to only
349 12 ± 2 hours at 0.15% LA. All systems were stable for considerably longer than foams
350 composed of pure surfactant solutions, which were only stable for 1.5 – 4 hours (Figure 6b).
351 A similar trend in foam stability is often seen for particle-surfactant systems where the most
352 stable foam corresponds to the optimum ratio of particle to surfactant concentration [5, 8,
353 44]. This is where particles are coated with a surfactant monolayer resulting in their lowest
354 charge and maximum hydrophobicity. Foam stability then decreases due to the formation of
355 a surfactant bilayer on the particle surface rendering them hydrophilic and resulting in the
356 mechanism of stabilisation changing from particle-stabilised to surfactant-stabilised. This
357 explanation does not justify the peak in foam stability observed here, as the ζ -potential data
358 (Figure 2) revealed that a bilayer did not form on the surface of particles at high LA
359 concentrations as particles remained negatively charged. To investigate the trend observed

360 here, the position of the particles in the foams was explored, as well as the rate of
361 coarsening and liquid drainage.



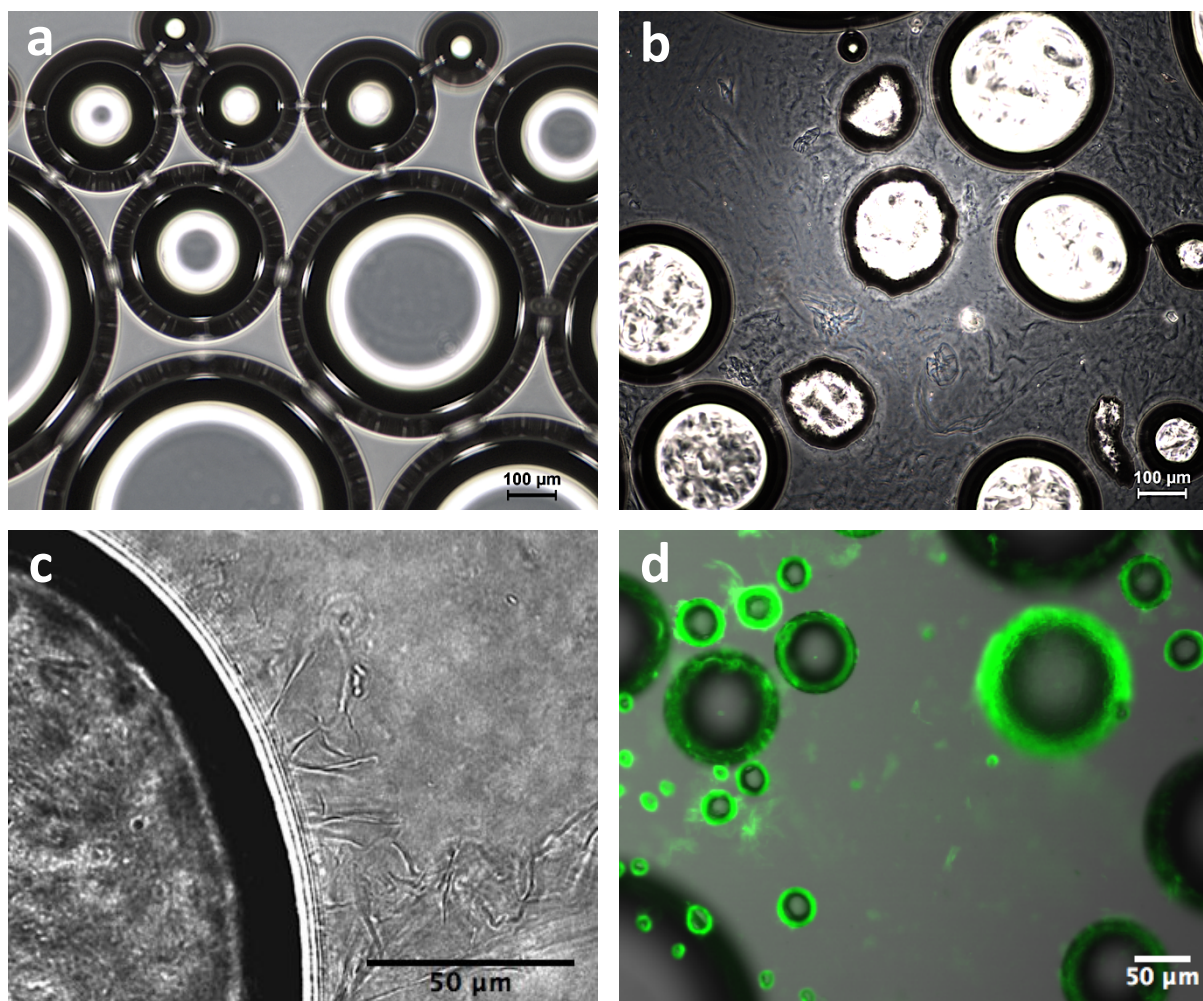
362
363 *Figure 6: (a) foam air fraction measurements for aerated κ C-LA complexes (■) and pure LA solutions (□), as a function of*
364 *LA concentration. Arrow indicates the CMC of LA. (b) foam half-life measurements for aerated κ C-LA complexes (■) and*
365 *pure LA solutions (□), as a function of LA concentration.*

366

367 3.5 Foam stability mechanism

368 Firstly, the location of particles in the foams was examined using optical and confocal
369 microscopy to investigate the surface-activity of the modified κ C particles. The bubbles
370 formed upon aerating pure LA solutions were also imaged for comparison; these bubbles
371 were spherical with smooth interfaces (Figure 7a). In contrast, foams produced with κ C-LA
372 complexes (at all LA concentrations) consisted of bubbles that appeared non-spherical and
373 had a structured surface (Figure 7b). This is indicative of bubbles stabilised by adsorbed
374 particles [8]. The micrograph in Figure 7c of aerated κ C with 0.075% LA further supports
375 this, as a layer of particulate entities can be seen at the surface of bubbles with tails
376 protruding into the continuous phase. Both micrographs (Figure 7b and Figure 7c) also
377 demonstrate the presence of particles in the continuous phase that had not adsorbed to the
378 interface. The particles appeared quite different to those imaged in Figure 1a before
379 complexation and aeration (longer and thinner in shape), it is possible that they deformed
380 to increase their efficiency of adsorption at bubble interfaces. To provide further
381 information on the coverage of bubble interfaces, confocal microscopy was used. Particles
382 were dyed with rhodamine B and appear green in the micrographs (Figure 7d). A layer of
383 particles can be seen on bubble interfaces providing high coverage. Particles can also be
384 seen in the continuous phase. Microscopy was used to study all aerated complexes; some
385 adsorption of particles at bubble interfaces was seen in all cases, verifying the ability to
386 surface-activate κ C particles through surfactant binding. However, it was difficult to
387 quantify the magnitude of particle coverage using microscopy. Therefore, the change in
388 bubble size over time was studied to analyse the effectiveness of particle coverage.

389



390
 391 *Figure 7: (a) optical micrograph of aerated 0.2% LA solution. (b) optical micrograph of aerated 1 wt% κ C + 0.075% LA fluid*
 392 *gel complexes. (c) optical micrograph of aerated 1 wt% κ C + 0.075% LA fluid gel complexes at a higher magnification. (d)*
 393 *confocal micrograph of aerated 1 wt% κ C + 0.075% LA fluid gel complexes dyed with rhodamine B.*

394

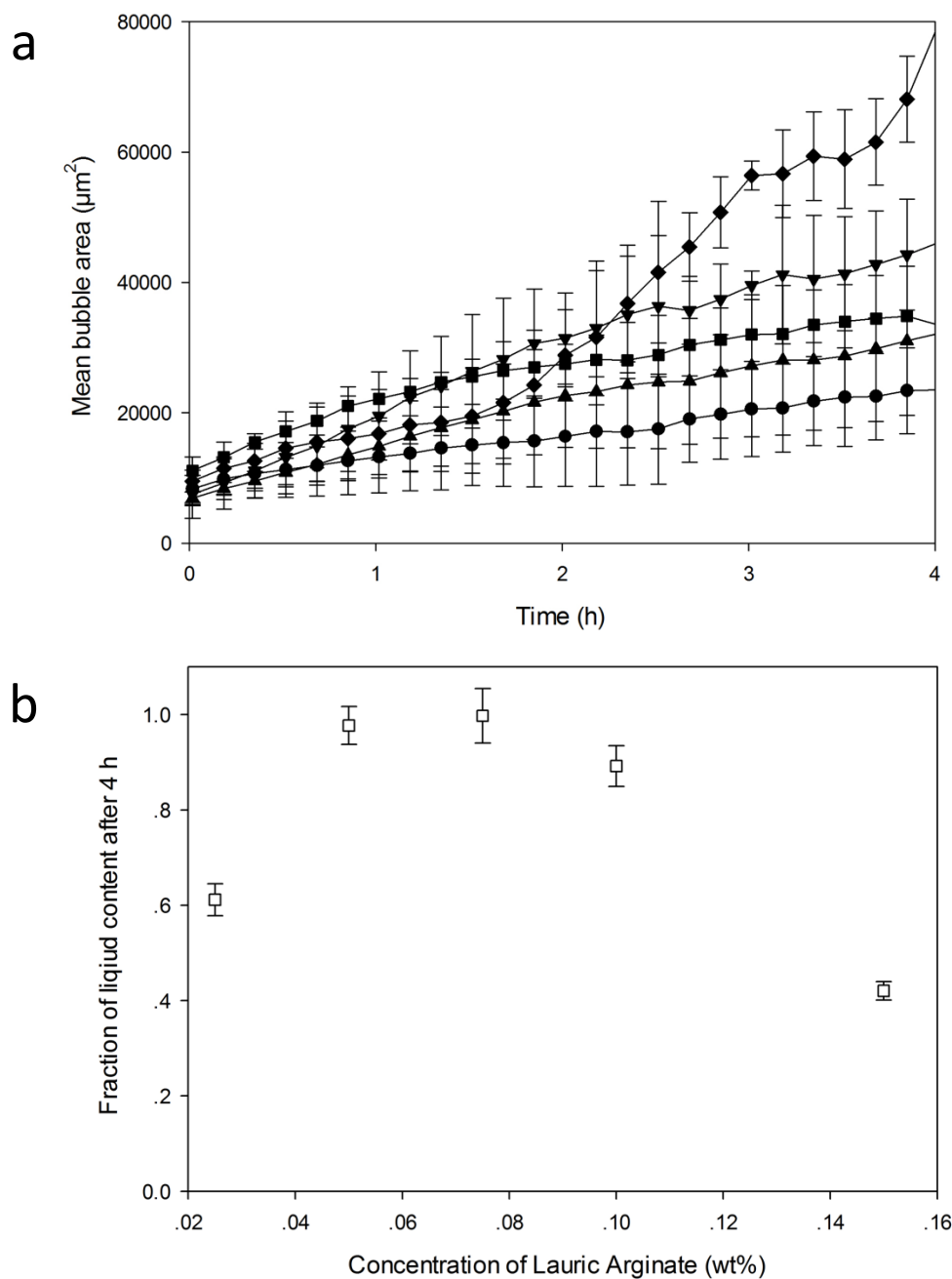
395 It has been well reported that particles adsorbed to a/w interfaces provide a barrier to
 396 coarsening of the gas phase [3, 22]. The structure of these foams including bubble size over
 397 time was therefore recorded using a high resolution camera. Mean bubble area as a
 398 function of time for the first 4 h after aeration was plotted for each foam (Figure 8a). The
 399 initial mean bubble area (MBA) was similar for all foams ($\sim 7000 \mu\text{m}^2$), which corresponds to
 400 a bubble radius of $\sim 12 \mu\text{m}$. The MBA increased with time in all cases, due to
 401 disproportionation. This is where smaller bubbles shrink in size and larger bubbles grow due
 402 to the difference in their internal Laplace pressure. The foam consisting of κ C particles and

403 0.025% LA displayed the highest rate of disproportionation (MBA $\sim 70000 \mu\text{m}^2$ after 4 h).
404 Upon increasing LA concentration to 0.05% and 0.075%, the smallest increase in MBA was
405 observed ($\sim 20000 \mu\text{m}^2$ after 4 h) and upon further increasing LA to 0.1% and 0.15%, the rate
406 of disproportionation subsequently increased again ($\sim 40000 \mu\text{m}^2$ after 4 h). These changes
407 in disproportionation rates suggest differences in interfacial viscoelasticity, perhaps caused
408 by a difference in stability mechanisms. It appears that at the lowest concentration of LA
409 (0.025%), the foam is surfactant stabilised and therefore more vulnerable to
410 disproportionation. At 0.05 and 0.075% LA, there is sufficient surfactant to coat the surface
411 of the particles and foams are consequently particle stabilised. The interfacial viscoelasticity
412 is high and the interface is protected against disproportionation. Above 0.075%, the rate of
413 disproportionation begins to increase again. This suggests a change in dominant stability
414 mechanism from particle stabilised to surfactant-stabilised. This cannot be due to the
415 formation of a surfactant bilayer and consequent change in particle charge as is common
416 with these systems (discussed in Section 3.4). It is therefore possible that there was a
417 barrier to adsorption for some of the particles. Deleurence, Parneix [37] studied the effect
418 of particle aggregation by de-coupling the effects of ζ -potential and particle charge (i.e. they
419 varied the sign of the ζ -potential without changing the contact angle over a large range of
420 surfactant concentration). They found that foam properties were controlled by the
421 flocculation state and the shear energy applied to produce the foam. Large aggregates did
422 not adsorb spontaneously at the interface because of their size, however, when large shear
423 energy was used to produce the foams, a very stable foam was formed. Adsorption of
424 particles occurs if the time for adsorption, t_A is considerably less than the time for interface
425 creation, t_{CR} . Both times depend on shear energy but the ratio does not. The ratio t_A/t_{CR}
426 scales as a/d , where a is the diameter of the particles and d is the diameter of the bubbles.

427 Large aggregates in the order of 100 μm could therefore not adsorb as $t_A/t_{CR}=10$. The size of
428 bubbles in this study were initially $\sim 12 \mu\text{m}$ (Figure 8a). Therefore when aggregates reached
429 $\sim 120 \mu\text{m}$ in diameter, adsorption would have been hindered. Above 0.075% LA, aggregates
430 greater than 100 μm in size were observed by optical microscopy, which continued to
431 increase in size with LA concentration (as discussed in Section 3.2). These would have been
432 unable to adsorb to the interface, which explains the trend seen in Figure 8a. The interface
433 would have been stabilised by free surfactant monomers, as well as those particles small
434 enough to adsorb (the number of which would have decreased with increasing LA
435 concentration).

436

437 As well as particles being present at a/w interfaces, microscopy highlighted their presence in
438 the continuous phase i.e. foam channels and nodes. Liquid drainage of the bulk phase was
439 therefore measured to assess how it related to foam stability. Liquid content, calculated
440 using conductivity data, is shown for each foam after 4 h as a fraction of initial content
441 (Figure 8b). The trend is similar to that observed for foam half-life. The particle stabilised
442 foams (0.05% LA and 0.07% LA) displayed little change in liquid content after 4 h. Whereas,
443 a decrease was measured for 0.025%, 0.1% and 0.15% LA (surfactant-stabilised foams). This
444 demonstrates that when particles adsorbed to the interface, their resistance to liquid
445 drainage as well as disproportionation increased. In addition, the interaction and
446 aggregation between particles would have helped to strengthen this barrier through the
447 formation of a particle network between air bubbles [7, 42, 45]. However, when foams were
448 surfactant stabilised, the classical drainage equation is applicable [46, 47]. Despite higher
449 viscosity of the continuous phase upon increasing LA concentration (Figure 4), the liquid
450 drainage was controlled by the change in stability mechanism.



451

452 *Figure 8: (a) mean bubble area of aerated κ C-LA complexes as a function of time after aeration, LA concentrations of*
 453 *0.025% (◆), 0.05% (●), 0.075% (▲), 0.1% (▼) and 0.15% (■). (b) fraction of liquid content remaining 4*
 454 *h after aeration in aerated κ C-LA complexes as a function of LA concentration. Measurements were recorded at sensor 3 in*
 455 *a Krüss foam column (positioned half way down the foam).*

456 3.6 κ C fluid gels with non-ionic surfactant

457 In order to confirm this change in surface-activity of kappa carrageenan upon binding to LA,

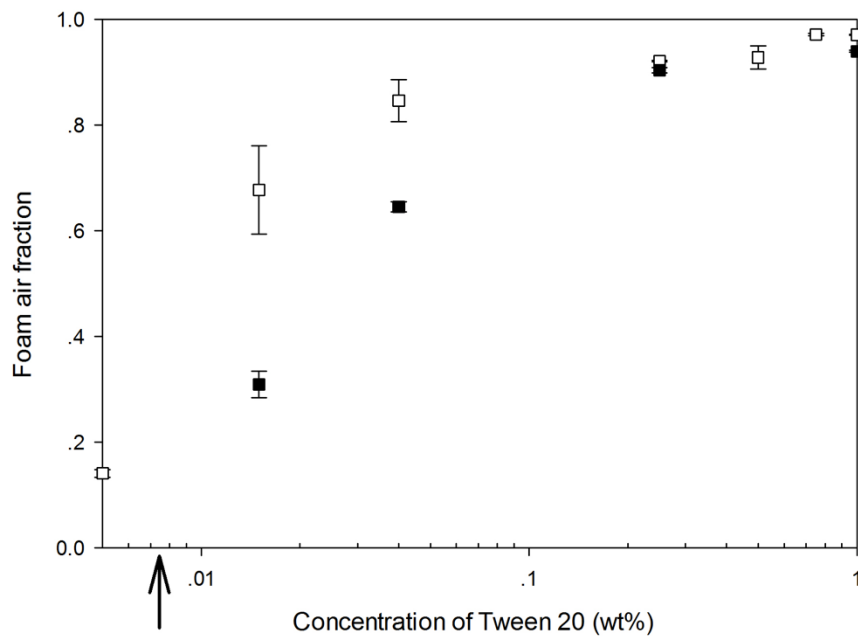
458 the foaming properties of kappa carrageenan mixed with a non-ionic surfactant, Tween 20,

459 were studied. Following the same procedure as LA, a diluted 1% κ C fluid gel was prepared

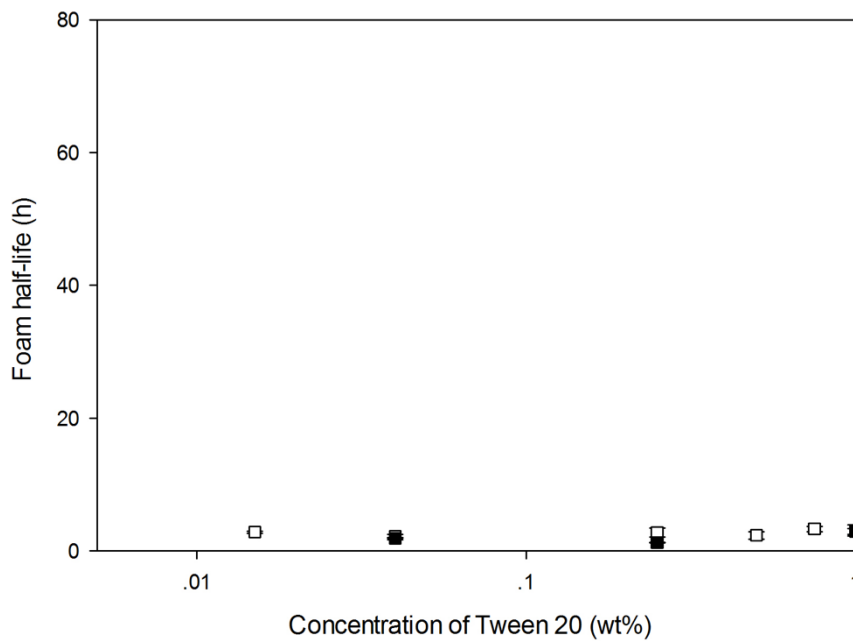
460 and mixed with Tween 20 at various concentrations. Firstly, their ability to incorporate air

461 was determined using foam air fraction measurements and compared to pure surfactant
462 solutions (Figure 9a). As the CMC of Tween 20 is quite low (0.0074 wt% [48]), which is
463 typical of non-ionic surfactants, it was used at concentrations above this in order to increase
464 foamability. The foam air fraction of pure surfactant solutions increased with Tween 20
465 concentration until it plateaued at around 0.98 (Figure 9a). Foam air fractions of κ C and
466 Tween 20 mixed solutions followed a similar trend but, as with κ C and LA fluid gel solutions,
467 they were slightly below those of pure Tween 20 due to increased viscosity. Foam half-lives
468 were then measured and plotted as a function of Tween 20 concentration in Figure 9b. No
469 increase in stability was observed upon addition of κ C to Tween 20 solutions; both systems
470 were stable for only 1-4 hours at all concentrations. In addition, the bubbles were spherical
471 and non-textured (Figure 9b inset), confirming that there was no adsorption of particles at
472 the interface or interaction between κ C and Tween 20.

a



b



473
474
475
476

Figure 9: (a) Foam air fraction measurements and (b) foam half-life measurements for 1 wt% κ C + Tween 20 fluid gel complexes (■) and pure Tween 20 solutions (□), as a function of Tween 20 concentration. Arrow in (a) indicates the CMC of Tween 20. (b) inset is an optical micrograph of aerated 1 wt% κ C + 0.075% Tween 20 fluid gel.

477 4 Conclusions

478 This research has built upon work by Bonnaud, Weiss [24] who characterised an
479 electrostatic interaction between food-grade cationic surfactant, lauric arginate, with
480 negatively charged carrageenan in solution but did not explore their surface properties or
481 ability to stabilise the a/w interface. In this work, the electrostatic interaction was facilitated
482 between microgel particles of kappa carrageenan and LA. Turbidity, ζ -potential and
483 rheological measurements were used to characterise the complexes, in particular their
484 aggregation behaviour, which showed similar patterns to those observed by Bonnaud,
485 Weiss [24]. The ability of complexes to lower surface tension was similar to that of pure
486 surfactant solutions, however foams were over 10 times more stable in all cases. Foam half-
487 life peaked at an intermediate concentration of LA (0.075% LA). This peak was attributed to
488 a change in stability mechanism from surfactant stabilisation to particle stabilisation, where
489 the most stable foams exhibited a smaller increase in mean bubble size over time (slower
490 disproportionation rate), as well as a slower liquid drainage rate. The adsorbed particles
491 therefore provided sufficient interfacial elasticity to considerably slow these mechanisms,
492 helped also by the interaction and aggregation between particles. However, at higher LA
493 concentrations, extensive aggregation limited their ability to adsorb to the interface and
494 foam stability decreased as surfactant stabilisation once again dominated. Similar particle-
495 surfactant systems have been limited by the formation of a surfactant bilayer on the surface
496 of particles, changing their hydrophobicity [5, 8, 44]. A surfactant bilayer did not form in this
497 system, suggesting that by optimising the size of particles and aggregates, greater foam
498 stability can be reached.

499

500 This work helps to expand the existing knowledge of *in-situ* modification of hydrophilic
501 particles for foam stabilisation, in particular work by Binks, Muijlwijk [14] who extended this
502 method to the food industry. To the best of the authors' knowledge, this is the first time
503 that a surfactant has been used to surface-activate kappa carrageenan particles facilitating
504 their adsorption to a/w interfaces. This provides a simple method to functionalise one of the
505 most commonly used polysaccharides in the food industry, providing a more versatile
506 ingredient for food microstructure design. For example, these particles have the potential to
507 mimic fat droplets in whipped products, in terms of both texture and their role in stabilising
508 the structure. There are many exciting future directions to further explore the knowledge
509 gained in this study. For example, the optimisation of microgel shape and size may allow
510 more efficient adsorption at the interface further increasing foam stability; Murphy, Farkas
511 [28] reported the ability of smaller microgel particles to adsorb to an interface and increase
512 interfacial elasticity more quickly. A more consistent shape and size may also allow the
513 adsorption kinetics and structure at the interface to be more thoroughly investigated. In
514 addition, the potential surface-activation of other polysaccharides (anionic and cationic)
515 with other surfactants should be explored to utilise this efficient method of modification.
516

517 **Acknowledgements**

518 This work was supported by the EPSRC Centre for Innovative Manufacturing
519 (EP/K030957/1).

- 520
- 521 1. Murray, B.S. and R. Ettelaie, *Foam stability: proteins and nanoparticles*. Current
522 Opinion in Colloid & Interface Science, 2004. **9**(5): p. 314-320.
- 523 2. Pickering, S.U., *Cxvii.—emulsions*. Journal of the Chemical Society, Transactions,
524 1907. **91**: p. 2001-2021.
- 525 3. Binks, B.P. and T.S. Horozov, *Aqueous foams stabilized solely by silica nanoparticles*.
526 Angewandte Chemie International Edition, 2005. **44**(24): p. 3722-3725.
- 527 4. Liu, Q., et al., *Aqueous foams stabilized by hexylamine-modified Laponite particles*.
528 Colloids and Surfaces A: Physicochemical and Engineering Aspects, 2009. **338**(1-3): p.
529 40-46.
- 530 5. Liu, Q., et al., *Foams stabilized by Laponite nanoparticles and alkylammonium*
531 *bromides with different alkyl chain lengths*. Colloids and Surfaces A: Physicochemical
532 and Engineering Aspects, 2010. **355**(1-3): p. 151-157.
- 533 6. Zhang, S., et al., *Aqueous foams stabilized by Laponite and CTAB*. Colloids and
534 Surfaces A: Physicochemical and Engineering Aspects, 2008. **317**(1-3): p. 406-413.
- 535 7. Gonzenbach, U.T., et al., *Stabilization of foams with inorganic colloidal particles*.
536 Langmuir, 2006. **22**(26): p. 10983-10988.
- 537 8. Cui, Z.G., et al., *Aqueous Foams Stabilized by in Situ Surface Activation of CaCO₃*
538 *Nanoparticles via Adsorption of Anionic Surfactant*. Langmuir, 2010. **26**(15): p.
539 12567-12574.
- 540 9. Rayner, M., et al., *Biomass-based particles for the formulation of Pickering type*
541 *emulsions in food and topical applications*. Colloids and Surfaces A: Physicochemical
542 and Engineering Aspects, 2014. **458**: p. 48-62.
- 543 10. Dickinson, E., *Double emulsions stabilized by food biopolymers*. Food Biophysics,
544 2011. **6**(1): p. 1-11.
- 545 11. Lam, S., K.P. Velikov, and O.D. Velev, *Pickering stabilization of foams and emulsions*
546 *with particles of biological origin*. Current Opinion in Colloid & Interface Science,
547 2014. **19**(5): p. 490-500.
- 548 12. Dickinson, E., *On the road to understanding and control of creaminess perception in*
549 *food colloids*. Food Hydrocolloids, 2017.
- 550 13. Ellis, A.L. and A. Lazidis, *Foams for food applications*, in *Polymers for Food*
551 *Applications*, T. Gutiérrez, Editor. 2018, Springer Publishing.
- 552 14. Binks, B.P., et al., *Food-grade Pickering stabilisation of foams by in situ*
553 *hydrophobisation of calcium carbonate particles*. Food Hydrocolloids, 2017. **63**: p.
554 585-592.
- 555 15. NHS. *Fat: the facts*. 2018 01/05/2017 15/10/18].
- 556 16. Katzbauer, B., *Properties and applications of xanthan gum*. Polymer degradation and
557 Stability, 1998. **59**(1-3): p. 81-84.
- 558 17. Chronakis, I.S. and S. Kasapis, *Food applications of biopolymer—theory and practice*,
559 in *Developments in food science*. 1995, Elsevier. p. 75-109.
- 560 18. Barclay, T., et al., *Inulin—a versatile polysaccharide with multiple pharmaceutical and*
561 *food chemical uses*. Journal of Excipients and Food Chemicals, 2016. **1**(3): p. 1132.
- 562 19. Norton, J.E. and I.T. Norton, *Designer colloids—towards healthy everyday foods?* Soft
563 Matter, 2010. **6**(16): p. 3735-3742.
- 564 20. Norton, I.T., T. Foster, and R. Brown, *The science and technology of fluid gels*. Special
565 publication-royal society of chemistry, 1998. **218**: p. 259-268.
- 566 21. Mori, I., *Vegan Society Poll*. 2016.

- 567 22. Dickinson, E., *Food emulsions and foams: Stabilization by particles*. Current Opinion
568 in Colloid & Interface Science, 2010. **15**(1–2): p. 40-49.
- 569 23. Benford, D., et al., *Safety Evaluation of Certain Food Additives: Ethyl Lauroyl*
570 *Arginate*. World Health Organization, Geneva, 2009.
- 571 24. Bonnaud, M., J. Weiss, and D.J. McClements, *Interaction of a food-grade cationic*
572 *surfactant (lauric arginate) with food-grade biopolymers (pectin, carrageenan,*
573 *xanthan, alginate, dextran, and chitosan)*. Journal of agricultural and food chemistry,
574 2010. **58**(17): p. 9770-9777.
- 575 25. Asker, D., J. Weiss, and D.J. McClements, *Formation and Stabilization of*
576 *Antimicrobial Delivery Systems Based on Electrostatic Complexes of Cationic–Non-*
577 *ionic Mixed Micelles and Anionic Polysaccharides*. Journal of Agricultural and Food
578 Chemistry, 2011. **59**(3): p. 1041-1049.
- 579 26. Dickinson, E., *Microgels — An alternative colloidal ingredient for stabilization of food*
580 *emulsions*. Trends in Food Science & Technology, 2015. **43**(2): p. 178-188.
- 581 27. Deshmukh, O.S., et al., *Equation of state and adsorption dynamics of soft microgel*
582 *particles at an air–water interface*. Soft matter, 2014. **10**(36): p. 7045-7050.
- 583 28. Murphy, R.W., B.E. Farkas, and O.G. Jones, *Dynamic and viscoelastic interfacial*
584 *behavior of β -lactoglobulin microgels of varying sizes at fluid interfaces*. Journal of
585 colloid and interface science, 2016. **466**: p. 12-19.
- 586 29. Destribats, M., et al., *Soft microgels as Pickering emulsion stabilisers: role of particle*
587 *deformability*. Soft Matter, 2011. **7**(17): p. 7689-7698.
- 588 30. Li, Z. and T. Ngai, *Microgel particles at the fluid–fluid interfaces*. Nanoscale, 2013.
589 **5**(4): p. 1399-1410.
- 590 31. Gabriele, A., F. Spyropoulos, and I.T. Norton, *A conceptual model for fluid gel*
591 *lubrication*. Soft Matter, 2010. **6**(17): p. 4205-4213.
- 592 32. Gabriele, A., F. Spyropoulos, and I.T. Norton, *Kinetic study of fluid gel formation and*
593 *viscoelastic response with kappa-carrageenan*. Food Hydrocolloids, 2009. **23**(8): p.
594 2054-2061.
- 595 33. de Carvalho, W. and M. Djabourov, *Physical gelation under shear for gelatin gels*.
596 Rheologica Acta, 1997. **36**(6): p. 591-609.
- 597 34. Asker, D., J. Weiss, and D.J. McClements, *Analysis of the Interactions of a Cationic*
598 *Surfactant (Lauric Arginate) with an Anionic Biopolymer (Pectin): Isothermal Titration*
599 *Calorimetry, Light Scattering, and Microelectrophoresis*. Langmuir, 2009. **25**(1): p.
600 116-122.
- 601 35. Morris, E., D.A. Rees, and G. Robinson, *Cation-specific aggregation of carrageenan*
602 *helices: domain model of polymer gel structure*. Journal of Molecular Biology, 1980.
603 **138**(2): p. 349-362.
- 604 36. Garrec, D.A., B. Guthrie, and I.T. Norton, *Kappa carrageenan fluid gel material*
605 *properties. Part 1: Rheology*. Food Hydrocolloids, 2013. **33**(1): p. 151-159.
- 606 37. Deleurence, R., C. Parneix, and C. Monteux, *Mixtures of latex particles and the*
607 *surfactant of opposite charge used as interface stabilizers–influence of particle*
608 *contact angle, zeta potential, flocculation and shear energy*. Soft Matter, 2014.
609 **10**(36): p. 7088-7095.
- 610 38. Saint-Jalmes, A., *Physical chemistry in foam drainage and coarsening*. Soft Matter,
611 2006. **2**(10): p. 836-849.

- 612 39. Moakes, R., A. Sullo, and I. Norton, *Preparation and characterisation of whey protein*
613 *fluid gels: The effects of shear and thermal history*. Food Hydrocolloids, 2015. **45**: p.
614 227-235.
- 615 40. Fernández Farrés, I., R.J.A. Moakes, and I.T. Norton, *Designing biopolymer fluid gels:*
616 *A microstructural approach*. Food Hydrocolloids, 2014. **42, Part 3**: p. 362-372.
- 617 41. Hunter, T.N., et al., *The role of particles in stabilising foams and emulsions*. Advances
618 in colloid and interface science, 2008. **137(2)**: p. 57-81.
- 619 42. Binks, B.P., *Particles as surfactants—similarities and differences*. Current Opinion in
620 Colloid & Interface Science, 2002. **7(1–2)**: p. 21-41.
- 621 43. Lesov, I., S. Tcholakova, and N. Denkov, *Factors controlling the formation and*
622 *stability of foams used as precursors of porous materials*. Journal of Colloid and
623 Interface Science, 2014. **426**: p. 9-21.
- 624 44. Guillermic, R.-M., et al., *Surfactant foams doped with laponite: unusual behaviors*
625 *induced by aging and confinement*. Soft Matter, 2009. **5(24)**: p. 4975-4982.
- 626 45. Dickinson, E., et al., *Factors controlling the formation and stability of air bubbles*
627 *stabilized by partially hydrophobic silica nanoparticles*. Langmuir, 2004. **20(20)**: p.
628 8517-8525.
- 629 46. Koehler, S.A., S. Hilgenfeldt, and H.A. Stone, *A generalized view of foam drainage:*
630 *experiment and theory*. Langmuir, 2000. **16(15)**: p. 6327-6341.
- 631 47. Saint-Jalmes, A., Y. Zhang, and D. Langevin, *Quantitative description of foam*
632 *drainage: Transitions with surface mobility*. The European Physical Journal E, 2004.
633 **15(1)**: p. 53-60.
- 634 48. Mittal, K., *Determination of CMC of polysorbate 20 in aqueous solution by surface*
635 *tension method*. Journal of pharmaceutical sciences, 1972. **61(8)**: p. 1334-1335.
636
637